Journal of Physics: Conference Series **590** (2015) 012058 doi:10.1088/1742-6596/590/1/012058

Analysis of Elastic Scattering of ^{8}He+^{208}Pb System at around the Coulomb Barrier Energies

M Direkci[1,2], Y Kucuk[2,3], and I Boztosun[2,3]

[1] Department of Physics, Bozok University, 66100, Yozgat, Turkey
[2] Department of Physics, Akdeniz University, 07058, Antalya, Turkey
[3] Nuclear Sciences and Application Center, Akdeniz University, 07058, Antalya, Turkey

E-mail: mikaildirekci@yahoo.com

Abstract. The elastic scattering angular distribution of ^{8}He+^{208}Pb system is investigated at E_{lab} = 22.0 MeV within the framework of Optical Model by using phenomenological and microscopic potentials. For the phenomenological Optical Model calculations, both real and imaginary parts of the complex nuclear potential have been chosen to have the Wood-Saxon shape. In the microscopic Optical Model calculations, we have used double folding procedure to calculate the real part of optical potential for different kinds of density distributions of ^{8}He. A comparative study of this system has been conducted for the fist time by using phenomenological and microscopic potentials. It is observed that large imaginary radius value due to the existence of long-range absorption mechanism acting at large distances provides a very good agreement between theoretical results and experimental data with small χ^2/N values.

1. Introduction

By the development of Radioactive-Ion Beam Facilities [1], exotic nuclei especially having large spatial matter radii and neutron skin structure [2] near the drip line has taken a great deal attention in recent years [3, 4, 5, 6]. So far, there have been few studies in determining the radii of the sensitivity of weakly-bound [6, 7] and tightly-bound nuclei near the Coulomb barrier [8, 9]. It is well known that determining the radial sensitivity of the nuclear potential is a considerable task in order to explain the angular distribution of the elastic scattering cross section [8, 9]. In this study, we have investigated the interaction of ^{8}He nucleus with ^{208}Pb heavy-stable target at incident energy of laboratory, E_{lab} = 22.0 MeV. There is only one experimental elastic scattering angular distribution data of ^{8}He+^{208}Pb system measured by Marquinez-Duran *et al.* [10] for this system just around the Coulomb barrier energy. For this incident energy limitation, we focus on contribution of extra two neutron ($2n$) to the absorption and also radial sensitivity of optical potential. Hence, instead of determining new optical model parameter set, we used the global optical potential parameter set of ^{6}He that was derived by Kucuk *et al.* [11] at low energies to compare the radial sensitivity of imaginary radius r_w and the effect of this imaginary radius to the absorption.

Our aim is to conduct phenomenological and microscopic optical model (OM) analysis for the realistic matter density distributions of ^{8}He. In the next section, we briefly explain the optical models: phenomenological optical model is explained in subsection 2.1 and microscopic one in subsection 2.2. In Section 3, we present our results depending on an extra $2n$ admixture to absorption mechanism of reaction. Our discussion and conclusions are given in section 4.

2. Optic Model Analysis

2.1. ***Phenomenological Optical Model***

^{8}He+^{208}Pb system has been investigated near the Coulomb barrier energy. We have used the optical model in the theoretical calculations and the total effective potential in our model consists of the Coulomb, centrifugal, and nuclear potentials as follows:

$$V_{total}(r) = V_{nuclear}(r) + V_{Coulomb}(r) + V_{centrifugal}(r) \tag{1}$$

In the total effective potential, the Coulomb and centrifugal potentials are well known. The Coulomb potential [12, 13, 14] due to a charge $Z_P e$ interacting with a charge $Z_T e$ distributed uniformly over a sphere of Radius R_C is given by

$$V_{Coulomb}(r) = \begin{cases} \frac{Z_P Z_T e^2}{r}, & r \geq R_C \\ \frac{Z_P Z_T e^2}{2R_C}(3 - \frac{r^2}{R_C^2}), & r < R_C \end{cases} . \tag{2}$$

where R_C is the Coulomb radius, taken as $R_C = 1.3(A_P^{1/3} + A_T^{1/3})$ fm in the calculations, Z_P and Z_T are defined as the charges of the projectile P and target T respectively. The centrifugal potential is

$$V_{centrifugal}(r) = \frac{\hbar^2}{2\mu}\frac{\ell(\ell+1)}{r^2}, \tag{3}$$

where μ is the reduced mass. Finally, the complex nuclear potential $V_{nuclear}(r)$ is taken to be the sum of both Woods-Saxon shaped $(W - S)$ real and imaginary potentials given as,

$$V_{nuclear}(r) = -\frac{V_0}{\left[1 + exp(\frac{r-R_v}{a_v}))\right]} - i\frac{W_0}{\left[1 + exp(\frac{r-R_w}{a_w})\right]} \tag{4}$$

Here, V_0, W_0 are reel and imaginary depth and the nuclear radius are $R_i = r_i(A_P^{1/3} + A_T^{1/3})$ $(i = v$ or $w)$, where A_P and A_T are the masses of projectile and target nuclei and r_v and r_w are the radius parameters of the real and imaginary part of the nuclear potentials respectively. We have used the code FRESCO [15] for the elastic scattering angular distribution calculations. The parameters of real and imaginary potentials are given in Table 1. All potential parameters except the radius of imaginary potential, r_w, are taken from Kucuk *et al.* [11]. The experimental data are taken from Ref. [16].

Table 1. Optical potential parameters for the ^{8}He+^{20}Pb system at $E = 22.0$ MeV

V_0 (MeV)	r_v (fm)	a_v (fm)	W_0 (MeV)	r_w (fm)	a_w (fm)	J_V $(MeV.fm^3)$	J_W $(MeV.fm^3)$	σ_R (mb)	χ^2/N
153.46	0.9	0.7	9.34	1.56	0.7	153.49	45.84	1535	0.29

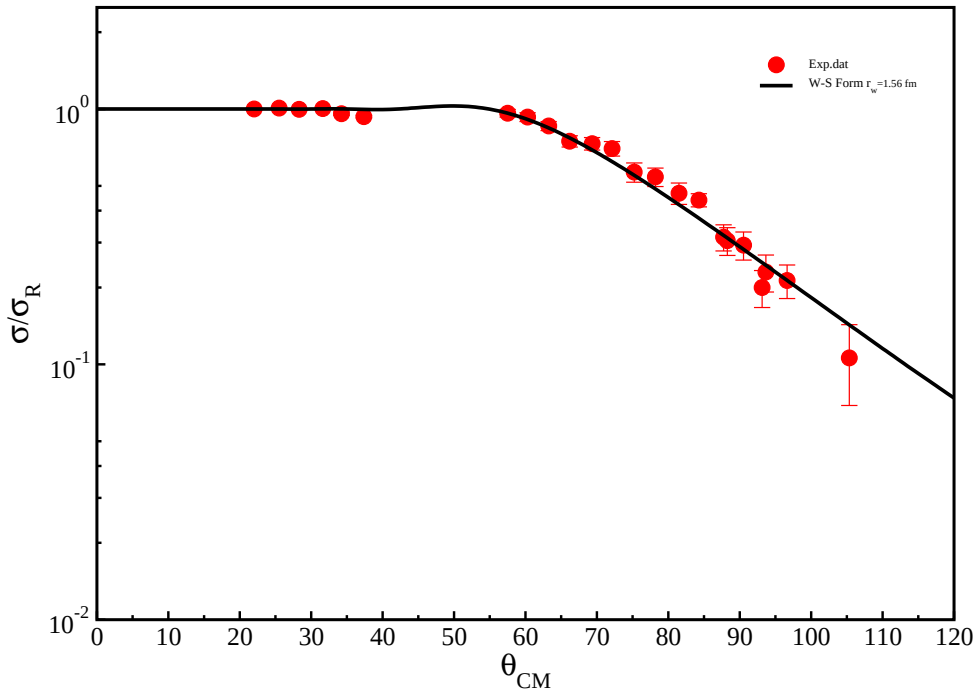

Figure 1. The angular distribution of the elastic scattering cross section of the ^{8}He+^{208}Pb system obtained with r_w=1.56 fm with χ^2/N=0.29.

2.2. ***Microscopic Optical Model***

In this part of theoretical calculations, we determined the real part of the complex $V_{nuclear}(r)$ potential by using the double-folding model. In order to calculate the double-folding potential, the nuclear matter distributions of both projectile ρ_P and target ρ_T nuclei together with an effective nucleon-nucleon interaction potential (υ_{NN}) are used. Hence, the double-folding potential is,

$$V_{DF}(\mathbf{r}) = \int d\mathbf{r_1} \int d\mathbf{r_2} \rho_P(\mathbf{r_1}) \rho_T(\mathbf{r_2}) \upsilon_{NN}(\mathbf{r_{12}}) \tag{5}$$

where ρ_P and ρ_T are the nuclear matter density of projectile and target nuclei respectively [20, 21]. In order to perform a comparative study, we have used three different matter density distributions for the ^{8}He ground state. First density distribution of ^{8}He structure was obtained by Tanihata *et al.* [17] in which Tanihata calculated ^{8}He density by using proton and neutron densities. Second one is obtained by Zhukov *et al.* [2] in which Zhukov applied the cluster-orbital shell-model ($COSMA$) approximation to the ^{8}He where ^{8}He consist of α core + ($4n$) parts. The last one is Symmetrize Fermi (SF) Model which was performed by Lukyanov *et al.* [18] in which $4n$ placed symmetrically around the α core. The detailed explanations of all density distributions of these models used in this study can be found in the relevant papers.

The effective nucleon-nucleon interaction, υ_{NN}, is integrated over both density distributions of ρ_P and target ρ_T nuclei. In literature, several nucleon-nucleon interaction expressions is used for the folding model potential calculations. We have chosen the most used one, M3Y nucleon-nucleon (Michigan3Yukawa) realistic interaction [19, 20, 21], that is given by

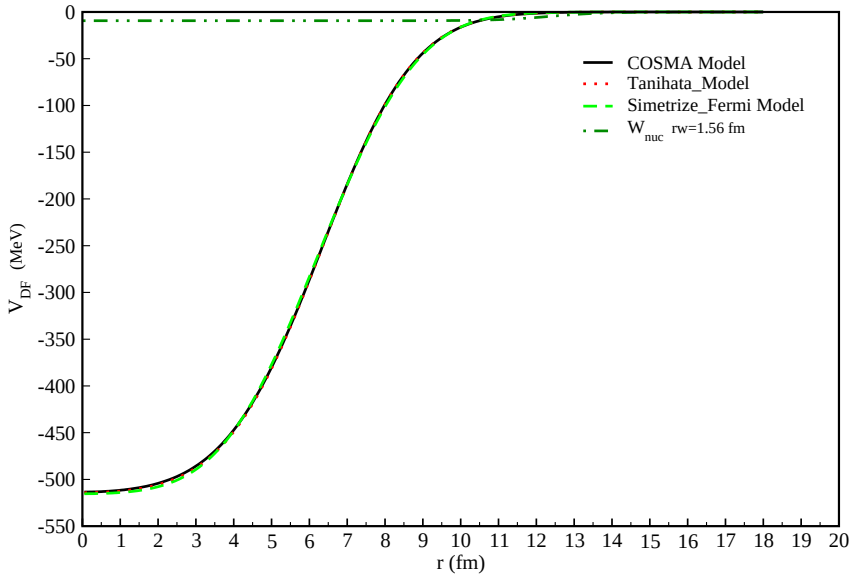

Figure 2. The real part of the nuclear potential obtained by three different density distributions by using the double folding model for ^{8}He. The imaginary part of nuclear potential with W-S form is also shown.

$$\upsilon_{NN}(r) = 7999\left[\frac{exp(-4r)}{4r}\right] - 2134\left[\frac{exp(-2.5r)}{2.5r}\right] + J_{00}(E)\delta(r)MeV \tag{6}$$

where $J_{00}(E)$ represents the exchange term since nucleon exchange is possible between the projectile and target. $J_{00}(E)$ has linear energy-dependence and defined as

$$J_{00}(E) = -276\left[1 - 0.005\frac{E_{lab}}{A_P}\right] MeVfm^3 \tag{7}$$

In the microscopical OM calculations, the real part of OM potential has been obtained by using above description of double-folding model, the imaginary potential has been taken as W-S form as mentioned above. Therefore, for the calculation of DF potential case, nuclear potential consists of real and imaginary parts, expressed as given by;

$$V_N(r) = N_R V_{DF}(r) - i\frac{W_0}{\left[1 + exp(\frac{r-R_w}{a_w})\right]} MeV \tag{8}$$

where N_R is the normalization factor and we fixed it as 1.0 for all DF calculations. The parameter set of DF calculations are shown in Table 2 and the double-folding potentials obtained by using above-mentioned three different density distributions together with the imaginary potential with r_w=1.56 fm are shown in Fig. 2. As it can be seen from this figure, all density distributions provide almost the same potentials around the Coulomb barrier energies. The angular distribution of elastic scattering of the system obtained by using these density distributions is shown in Fig. 3. For the density distribution of ^{208}Pb, we has used the density of $RIPL-2$ [22].

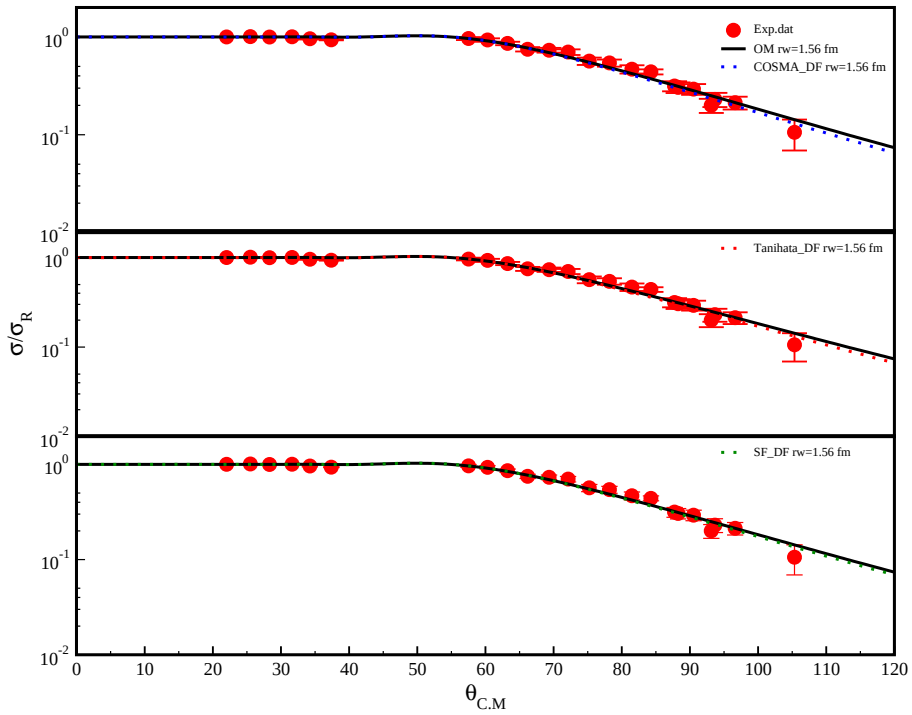

Figure 3. The angular distribution of the elastic scattering cross section of the ^{8}He+^{208}Pb system obtained with r_w=1.56 fm with $\chi^2/N = 0.20$.

The real and imaginary potentials have been studied in terms of their volume integrals in our study. We also show the tabulated values of the real and imaginary volume integrals (J_V and J_W) per interacting nuclear pair in Table 1 and Table 2 and the volume integrals defined as

$$J_{V,W} = \frac{4\pi}{A_p A_T} \int_0^\infty U_{V,W}(r) r^2 dr \tag{9}$$

where A_p and A_T are the projectile and target masses. Reaction cross-section of these three density distributions are also shown in Table 2. They predict similar values around around 1550 mb.

Table 2. The parameters of ^{8}He+^{208}Pb system and their cross section predictions, χ^2/N values and volume integrals. $N_R = 1.0$ is fixed for all calculations.

Density Model	W_0 (MeV)	r_w (fm)	a_w (fm)	J_V $(MeV.fm^3)$	J_W $(MeV.fm^3)$	σ_R (mb)	χ^2/N
COSMA	9.34	1.56	0.7	417.68	45.84	1554	0.20
Tanihata	9.34	1.56	0.7	417.76	45.84	1551	0.22
SF	9.34	1.56	0.7	417.68	45.84	1546	0.23

3. Results

By using the above-described phenomenological and microscopic potentials, we have investigated the elastic scattering of ^{8}He+^{208}Pb system at E_{lab} = 22.0 MeV. In order to explain the data,

we have to modify the radius of the imaginary potential of Kucuk *et al.* [11] as $r_w = 1.56$ fm. The parameters of the potentials for phenomenological and microscopic potentials are given in Table 1 and Table 2 respectively. The result of phenomenological potential calculations is shown in Fig. 1 and it can be seen from this figure that the agreement is very good over the whole angular range in comparison with the experimental data. The results of microscopic potentials obtained with the three different density distributions are shown in Fig. 3. The results are also in very good agreement with the experimental data. Both phenomenological and microscopic potentials predict similar reaction cross-section values around 1550 mb. Volume integrals of both phenomenological and microscopic potential are also calculated and the values are given in Table 1 and Table 2. The volume integral for the real part of the microscopic potential is much larger than the phenomenological one.

4. Discussion and Conclusions

We have studied the elastic scattering of ^{8}He neutron-skin nucleus from a heavy-stable ^{208}Pb target. We have used both phenomenological and microscopic potentials to explain the experimental data. Phenomenological potentials have the W-S shape for both real and imaginary parts. Three different density distributions in the double-folding model are used for the real part of microscopic potential calculations. We have observed three different density distributions proposed to define the density of ^{8}He provide almost the same real potential around Coulomb barrier. We also noticed that the radius of imaginary potential should be large enough to obtain correct absorption. Both phenomenological W-S potential and microscopic calculations with three different density distribution provide a good agreement with the experimental data with phenomenological W-S imaginary potential. The OM calculations for other reaction systems are still in progress.

Acknowledgments

This work was partly supported by the scientific research projects units of Bozok and Akdeniz Universities.

References

[1] Ter-Akopian G M *et al.* 2004 *Nucl. Phys.* A **734** 295
[2] Zhukov M V Korsheninnikov A A and Smedberg M H 1994 *Phys. Rev.* C **50** 1
[3] Tanihata I *et al.* 1995 *Prog. Part. Nucl. Phys.* **35** 505
[4] Tanihata I *et al.* 1996 *J. Phys. G: Nucl. Part. Phys.* **22** 157
[5] Thompson I J and Suzuki Y 2001 *Nucl. Phys.* A **693** 424
[6] Jonson B 2004 *Phys. Rep.* **389** 1
[7] Rusek K *et al.* 2004 *Phys. Rev.* C **70** 014603
[8] Mazzocco M *et al.* 2014 *Act. Phys. Pol.* B **45** 2
[9] Biswas M 2008 *Phys. Rev.* C **77** 017602
[10] Marquinez G-Duran *et al.* 2012 *Act. Phys. Pol.* B **43** 2
[11] Kucuk Y, Boztosun I and Topel T 2009 *Phys. Rev.* C **80** 054602
[12] Satchler G R 1983 *Direct Nuclear Reactions* (Oxford,Oxford University Press)
[13] Boztosun I and Rae WDM 2001 *Phys. Lett.* **518B** 229
[14] Boztosun I 2002 *Phys. Rev.* C **66** 024610
[15] Thompson I 1988 *J. Comput. Phys. Rep.* **7** 167
[16] Experimental Nuclear Reaction Data ($EXFOR$) 2011 *Database Version of November 02*
[17] Tanihata I 1992 *Phys. Lett.* B **289** 261
[18] Lukyanov V K *et al.* 2003 arXiv:nucl-t/0311040v1
[19] Satchler G R and Love W G 1979 *Phys. Rep.* **55** 183
[20] Karakoc M and Boztosun I 2006 *Phys. Rev.* C **73** 047601
[21] Karakoc M and Boztosun I 2006 *Int. J. of Mod. Phys.* E **15** 1317
[22] Reference Input Parameter Library ($RIPL-2$), http://www.nds.iaea.org/RIPL-2/